

VARIATIONS IN THE ABUNDANCE OF SMALL PARTICLES

F. BOULANGER

*Radioastronomie, Ecole Normale Supérieure,
24 rue Lhomond, 75005 Paris, France*

Abstract. IRAS images of nearby molecular clouds show that the mid-IR emission from small particles in the size range 10^2 to 10^5 atoms is distributed very differently from the $100\ \mu\text{m}$ emission from large dust grains. Variations in color ratios by as much as one order of magnitude are seen on all angular scales. We summarize observational properties of the color variations and argue that neither their large amplitude nor their morphology can be explained by changes of the excitation by the UV radiation field only. The color variations reflect considerable inhomogeneities in the abundance of small particles. We suggest that the abundance variations are related to the cycling of interstellar matter between the gas phase and dust grains. This interpretation entails that clouds with distinct IR colors differ in their density and velocity structure and that cycling of matter between gas phase and dust grains is more ubiquitous and rapid than generally thought.

Keywords : Molecular Clouds, Grains : Size Distribution, IR Emission, IRAS Colors

1. Introduction

IRAS images of nearby molecular clouds at the four wavelengths 12, 25, 60, and $100\ \mu\text{m}$ provide a wealth of information on the composition of interstellar matter which has just begun to be analyzed. Particles contributing to the observed emission differ from one wavelength to the next. While the $100\ \mu\text{m}$ comes from large grains in thermal equilibrium with the radiation field, the 12 and $25\ \mu\text{m}$ emission, and, probably, part of the $60\ \mu\text{m}$ emission is radiated by particles with sizes in the range 0.5 to 10 nm for which the time between photon absorption is larger or comparable to the cooling time (Puget et al. 1985, Draine and Anderson 1985, Chlewicki and Laureijs 1988, Désert, Boulanger, and Puget 1990, hereafter DBP). These particles emit most of their emission at temperatures close to the peak temperature they reach after photon absorption. Since this temperature depends on the size of the particle, the spectral distribution of their IR emission is related to their size distribution (see Puget and Léger 1989). In their model DBP show that at least three dust components are needed to account for the IRAS data : (1) large molecules or cluster of molecules with one to a few hundred atoms (near-IR, 12 and part of $25\ \mu\text{m}$ emission), (2) very small dust grains with 10^3 to 10^5 atoms ($25\ \mu\text{m}$ and part of $60\ \mu\text{m}$ emission), and (3) dust grains with sizes larger than 10 nm in thermal equilibrium ($100\ \mu\text{m}$ and sub-mm emission). In practice the IRAS color ratios $R(12, 100) = I_\nu(12\ \mu\text{m})/I_\nu(100\ \mu\text{m})$, $R(25, 100) = I_\nu(25\ \mu\text{m})/I_\nu(100\ \mu\text{m})$ and $R(60, 100) = I_\nu(60\ \mu\text{m})/I_\nu(100\ \mu\text{m})$ measure the relative abundances of these three families of particles.

Early in the analysis of IRAS data on nearby clouds heated by the general interstellar radiation field of the Galaxy (ISRF), it appeared that the ratio between mid-IR (12 and $25\ \mu\text{m}$) and $100\ \mu\text{m}$ emission varies widely from cloud to cloud

(Boulanger et al. 1985, Leene 1985, de Vries and Le Poole 1985, Weiland et al. 1986, Boulanger and Pérault 1988, Heiles, Reach, and Koo 1988, Laureijs, Mattila, and Schnur 1987, Laureijs, Chlewicki, and Clark 1988, Beichman et al. 1988). Later, Boulanger (1989), Boulanger et al. (1989) and Puget (1989) stressed the existence of considerable variations (up to one order of magnitude) in IR colors on scales as small as the IRAS resolution (a few tenths of a parsec) within clouds in the complexes of Chamaeleon, Taurus, Ursa Major and Ophiuchus. Color variations within the first three complexes have been described in detail by Boulanger, Falgarone, Puget and Helou (1990, hereafter BFPH). Based on this work and preliminary comparison of IR images with molecular observations, we summarize observed properties of the color variations. Following BFPH we argue that the color variations reflect inhomogeneities in the abundance of small particles within and among clouds. Through the paper the dust model of DBP is used to discuss the excitation of small particles and quantify the abundance variations.

2. Observational Properties

2. 1. COLOR-BRIGHTNESS DIAGRAMS

Much can be learned on the variations of IR colors in molecular clouds by simply looking at the color images and cuts presented by BFPH, Boulanger (1989), Boulanger et al. (1989) and Puget (1989). To quantify these data, BFPH measured the IR brightnesses at the four IRAS wavelengths for several tens of positions within Chamaeleon, Taurus, and Ursa Major. Along most of the selected lines of sight $A_v < 2\text{mag}$. The colors computed at these positions are presented in figure 1 in three diagrams, R(12,25), R(12,100) and R(60,100) versus $I_\nu(100\mu\text{m})$. In these diagrams $I_\nu(100\mu\text{m})$ may be considered as a measure of the total column density along the line of sight. Direct comparisons of $I_\nu(100\mu\text{m})$ with A_v in Taurus and Chamaeleon show a good correlation for $A_v < 3\text{mag}$ with a slope of 5 - 10 (MJy/sr)/mag, independent of the IR colors of the cloud.

The main feature of the diagrams is the considerable scatter of the R(12,100) and R(60,100) colors at all $I_\nu(100\mu\text{m})$. Values of R(12,100) range from ~ 0.008 to 0.2, 1/5 to 5 times the average value for atomic gas in the Solar Neighborhood (Boulanger and Pérault 1988). Matter with a high $12\mu\text{m}$ emissivity, defined by a R(12,100) color higher than the average Solar Neighborhood value is observed only in the external parts of clouds. The $100\mu\text{m}$ brightness associated with this matter is at most 10 MJy/sr which corresponds to an A_v of 1 mag. This important property of the color variations translates in the diagram of figure 1 by a general decrease of R(12,100) with increasing $I_\nu(100\mu\text{m})$. The median value of R(12,100) decreases from 0.14 for $I_\nu(100\mu\text{m}) \sim 2\text{MJy/sr}$, to 0.07 at $I_\nu(100\mu\text{m}) \sim 5\text{MJy/sr}$, and 0.03 for $I_\nu(100\mu\text{m})$ between 10 and 20 MJy/sr. Values of R(12,100) larger than 0.05 for $I_\nu(100\mu\text{m}) > 10\text{MJy/sr}$ can all be ascribed to bright envelopes of $12\mu\text{m}$ emission. In each of these cases no $12\mu\text{m}$ emission is seen from the inner parts of the cloud, $I_\nu(12\mu\text{m})$ is limb-brightened and is minimal at the position where $I_\nu(100\mu\text{m})$ peaks.

$R(60,100)$ is observed to vary from 0.05 to 0.3, the average Solar Neighborhood value being 0.2. This color appears roughly independent of $I_\nu(100\mu\text{m})$. Within a cloud, variations in $R(60,100)$ and $R(12,100)$ are often correlated (Beichman et al. 1988) but this is not a systematic feature (Laureijs, Chlewicki and Clark 1988). The correspondence between these two colors is clearly not universal: it varies from cloud to cloud.

By contrast to the two other colors in figure 1, $R(12,25)$ is remarkably constant. Taking into account uncertainties on the measurements the real scatter of $R(12,25)$ is about a factor of 2, one order of magnitude smaller than that observed for $R(12,100)$. This result suggests a close correlation between the populations of particles generating the 12 and $25\mu\text{m}$ emission. This is not a trivial result since dust models predict that only half of the $25\mu\text{m}$ emission is coming from particles giving rise to the $12\mu\text{m}$ emission (Chlewicki and Laureijs 1988, DBP).

2. 2. MORPHOLOGY AND PHYSICAL PROPERTIES

In view of the IRAS images, without oversimplifying the data we may distinguish three kinds of clouds. (1) Clouds with uniformly little or no 12 and $25\mu\text{m}$ emission (e.g. Cha I and III in Chamaeleon, L1495 and 1506 in Taurus), (2) clouds with an envelope of bright 12 and $25\mu\text{m}$ emission around more opaque pieces with no 12 nor $25\mu\text{m}$ emission (e.g. G300-15 in Chamaeleon, Heiles 2, B5), (3) clouds with randomly distributed IR colors (e.g. Ursa Major, L1497 and 1541). In this last type of clouds the spread of IR colors is generally smaller than the full range of colors observed between clouds of types (1) and (2). In Chamaeleon, matter with $R(12,100)$ larger than the average Solar Neighborhood value accounts for 1/3 of the total $100\mu\text{m}$ emission of the complex. This emission fraction translates into a comparable (little smaller) fraction of the total mass of the complex. In the two other complexes the different types of clouds are not separated enough to make a similar estimate.

Clouds of type (1) have no noticeable envelope with warmer IR colors. Preliminary comparisons of CO and $100\mu\text{m}$ emission in a few of these clouds show that CO is detected all the way to the edge of the $100\mu\text{m}$ emission (see figure 2).

The peak column density through the envelopes with high $R(12,100)$ characteristic of clouds of type (2), as measured from $I_\nu(100\mu\text{m})$ or directly from star counts, corresponds to $A_\nu < 1\text{mag}$. Images and cuts (BFPH, Boulanger 1989, and Puget 1989) illustrate the variety of morphologies of regions of high $R(12,100)$. Their linear projected size varies from 0.3 pc to 10 pc. Based on the $100\mu\text{m}$ brightness and the cloud geometry the density of the gas emitting strongly at $12\mu\text{m}$ is estimated to be one to a few 100Hcm^{-3} . CO observations for several clouds in different complexes indicate that this gas is not seen in emission in CO (see example in figure 2). For a few stars in Chamaeleon, absorption spectra were taken through this gas leading to the detection of CH (Boulanger et al. in preparation) which indicates the presence of H_2 . Within many clouds of type (2) the color transition is unresolved by IRAS so that the size of the transition region is $< 0.2\text{pc}$. One example of such a

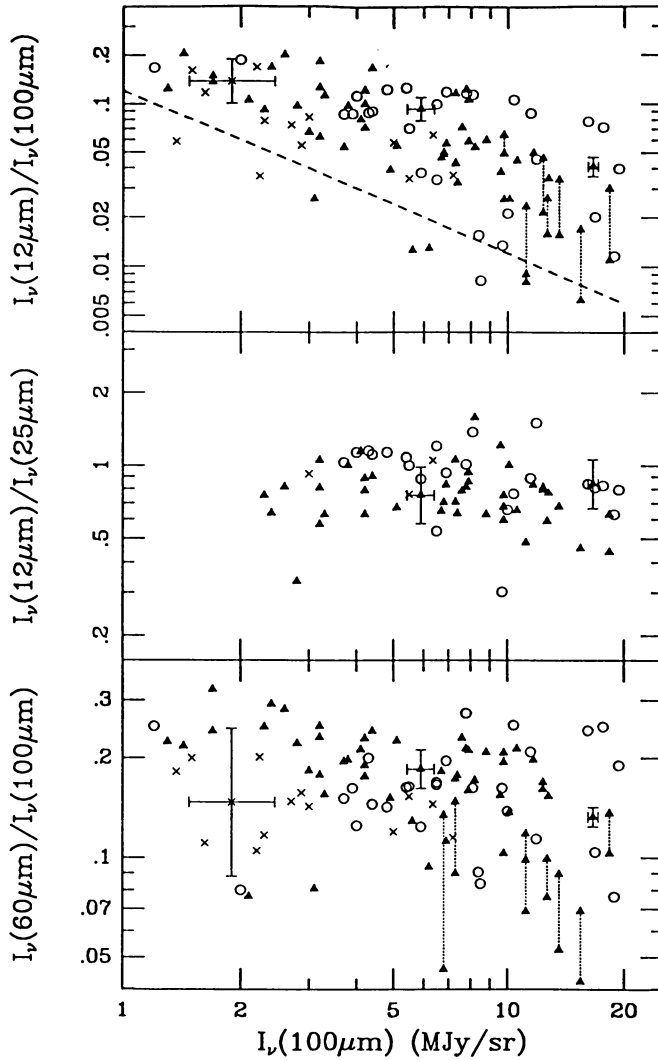


Fig. 1: (a) Plot of the color ratio $R(12,100) = I_\nu(12\mu\text{m})/I_\nu(100\mu\text{m})$ versus $I_\nu(100\mu\text{m})$. The symbols are circles for Chamaeleon, solid triangles for Taurus, and crosses for Ursa Major. The dashed line shows the sensitivity limit for measurements of the $12\mu\text{m}$ brightness. All data points near this line are upper limits on $R(12,100)$. For a few positions we measured the colors for two baselines: a global one defined for the whole cut and one defined locally from local minima of emission near the position of the measurements. The corresponding pairs of data points are connected by a dotted line (shown also on the $R(60,100)$ diagram). The smaller value $R(12,100)$ and $R(60,100)$ always correspond to the local baseline. Error bars are only given for three data points selected as representative of points with low, average, and high $I_\nu(100\mu\text{m})$. (b) Plot of $R(12,25)$ versus $I_\nu(100\mu\text{m})$. Only data points with $I_\nu(25\mu\text{m}) > 0.25 \text{ MJy/sr}$ are included.

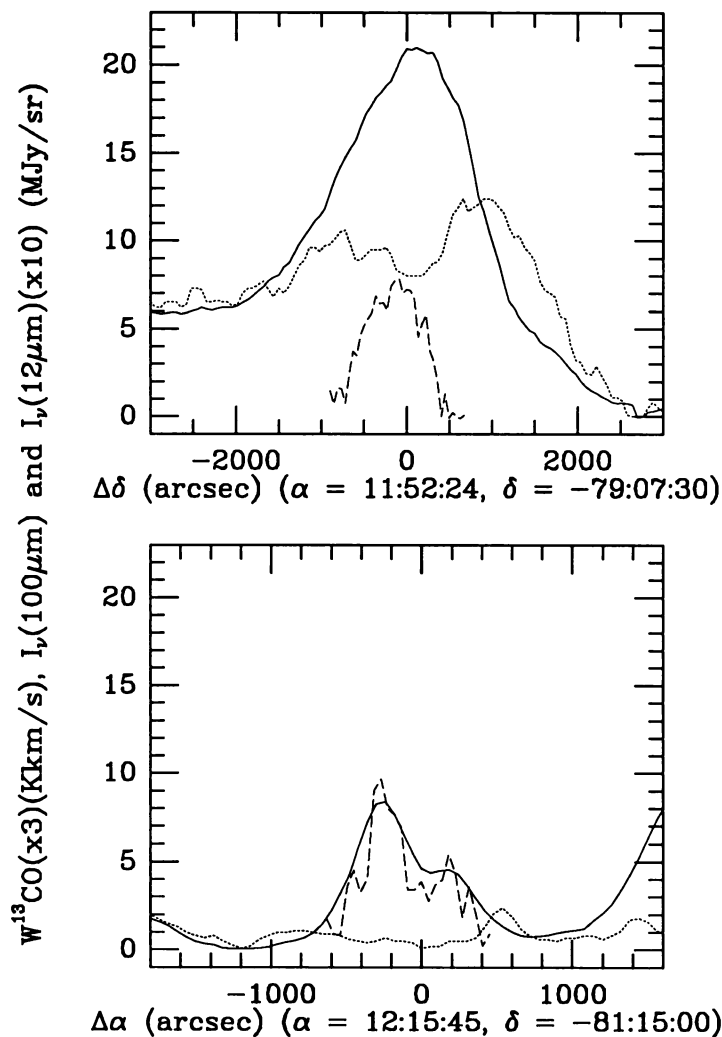


Fig. 2: $I_\nu(12\mu\text{m})$ (dotted line), $I_\nu(100\mu\text{m})$ (solid line), and $W(^{13}\text{CO})$ ($J=1-0$) (dashed line) cuts across two clouds in Chamaeleon. Relative scaling factors between the three brightnesses are the same in the two figures. The molecular data was obtained with the SEST (Boulanger et al. in preparation). The first cloud (left figure) shows strong $12\mu\text{m}$ emission from the outer parts of the cloud with a minimum at the peak of the $100\mu\text{m}$ emission. The molecular and IR data are consistent with all of the ^{13}CO emission coming from a central core of the cloud with no $12\mu\text{m}$ emission and a $100\mu\text{m}/^{13}\text{CO}$ emission ratio similar to that observed for the second cloud in the right figure. This cloud shows no $12\mu\text{m}$ emission and ^{13}CO emission all the way to the edge of the $100\mu\text{m}$ emission.

sharp transition is shown in figure 1 (cut 2) of Boulanger (1989). Other examples are L134 and L1780 studied by Laureijs, Clark and Prusti (1990). This sharpness may be a general feature only perceivable in clouds with a favorable geometry and orientation with respect to the observer. Existing molecular data and recent observations made with the SEST show that the color variations correlate with strong changes in gas density. Based on ^{13}CO J=2-1 and 1-0, and CS J=2-1 observations Boulanger et al. (in preparation) estimate the density of the gas not seen at 12 and $25\mu\text{m}$ to be $\sim 510^3\text{cm}^{-3}$, a factor 50 larger than that of the gas with high R(12,100).

3. Excitation by UV Light

On average over a whole molecular complex, the emission from small particles at $\lambda < 25\mu\text{m}$ is $\sim 10^{-31}\text{W}$ per hydrogen atoms. This represents roughly 25% of the total power radiated by the clouds in the infrared and sub-millimeter. It is difficult to imagine a source of energy other than star light which could contribute for any significant fraction of this emission. For example the energy per nucleon associated with turbulent motions is for a cloud of size D , using the line width - size relation $\Delta V(\text{FWHM}) = (D/1\text{pc})^{0.5}\text{km/s}$, $E_c = \frac{3}{2}\sigma_v^2 = 3(D/10\text{pc})10^{-21}\text{J/H}$. If shocks associated with turbulent motions in clouds were at the origin of the emission from small particles the turbulent energy will be dissipated in $\sim 10^3\text{yrs}$. No known mechanism is able to re-supply the turbulent energy of clouds at this rate. The emission from small particles is also higher than the heating rate of gas by photo-electrons by two orders of magnitude. Hence collisional excitation cannot be significant unless some unknown heating mechanism of the gas is active. Stellar light appears thus as the only possible source of excitation.

The small particles which have been proposed to account for the near and mid-IR emission from the interstellar medium absorb mostly in the ultraviolet (UV) (see Puget and Léger 1989). The variations of the mid-IR to far-IR emission ratio could thus result from changes in the rate of excitation of the small particles related to anisotropy and intensity variations in the UV radiation field. Beichman et al. (1988), Chlewicki and Laureijs (1988), and Laureijs et al. (1989) suggested that UV attenuation could account for the limb brightening of the $12\mu\text{m}$ emission seen across some clouds. Models to test quantitatively this idea have been presented by these authors and DBP. Even in the most favorable case where large grains absorb a large fraction of their energy in the red due to the formation of mantles the decrease of R(12,100) with increasing $I_\nu(100\mu\text{m})$ is only one tenth of the systematic decrease seen in figure 1 (BFPH). The model predicts small changes in R(12,100) because the attenuation of the UV radiation field reduces the 12 and $100\mu\text{m}$ emission at roughly the same rate. Since large grains absorb over the whole ISRF spectrum, attenuation of the UV part of the radiation field reduces their bolometric emission and temperature. The temperature decrease makes the reduction in the $100\mu\text{m}$ emission larger than that of the dust heating. This reduction

of the $100\mu\text{m}$ emission predicted by the model and which is important to dismiss excitation changes as the cause of color variations is verified by $I_\nu(100\mu\text{m}) - A_v$ comparisons. It corresponds to the reduction by a factor 2 to 3 observed in the $I_\nu(100\mu\text{m})/A_v$ ratio between atomic gas and molecular clouds (Boulanger 1989). Thus, models which fail to explain the limb brightening of the 12μ emission, do reproduce the observed decrease in the slope of the $100\mu\text{m} - A_v$ relation from atomic gas to molecular clouds (Chlewicki and Laureijs 1988, Bernard 1990).

Changes in the rate of UV excitation of the small particles are also inadequate in explaining the scatter of $R(12,100)$ observed in figure 1 at any given $I_\nu(100\mu\text{m})$. Again, to increase or decrease the $R(12,100)$ color of a cloud of a given opacity by some factor, the UV radiation field at its surface must be increased or decreased by a much larger factor because large grains emitting at $100\mu\text{m}$ also absorb in the UV. For example, in the calculations of Laureijs (1989) and DBP it is necessary to scale the UV part of the ISRF by a factor of ~ 5 to increase $R(12,100)$ by 50%. Such a change in the radiation field implies an increase of the $100\mu\text{m}$ emissivity per dust grain measured by the ratio $I_\nu(100\mu\text{m})/A_v$ of 3. The interpretation of the scatter in $R(12,100)$ at a given $I_\nu(100\mu\text{m})$ in Fig. 1 along this line would imply that the radiation field at the surface of the clouds varies by more than one order of magnitude from cloud to cloud. Such large inhomogeneities in the UV radiation field are completely excluded for the Chamaeleon, Taurus, and Ursa Major complexes which are located far-away from any OB association. While shadow effects between clouds can create regions of attenuated radiation field, UV radiation fields an order of magnitude more intense than the average ISRF, necessary to explain the high values of $R(12,100)$, cannot be obtained without nearby O or early B stars. Further, such an interpretation would imply variations of $I_\nu(100\mu\text{m})/A_v$ by more than an order of magnitude, correlated with those of $R(12,100)$, which are excluded by comparisons between A_v and $I_\nu(100\mu\text{m})$ (BFPH).

As for the $R(12,100)$, variations in the spectrum and strength of the radiation field are inadequate in explaining the variations in the $R(60,100)$ colors. For grains in thermal equilibrium the total amplitude of the $R(60,100)$ variations corresponds to a change in the intensity of the radiation field by a factor of 20 (DBP), larger than what is believable for complexes located far away from OB associations and for clouds with moderate opacity to star light. The scatter in $R(60,100)$ could be due to the contribution of small particles to the $60\mu\text{m}$ emission. Laureijs, Clark and Prusti (1990) have suggested that the formation of mantles on small particles could make them big enough to reduce their temperature fluctuation. For large grains the formation of mantles implies a change in optical properties and consequently in equilibrium temperature which could play a role in the $R(60,100)$ color variations.

4. Abundance Variations

Since changes in the UV field are ineffective in affecting IR colors the $R(12,100)$ and $R(25,100)$ color variations must reflect changes in the abundance of small particles. The importance of this conclusion comes from the large amount of material

necessary to account for the mid-IR emission measured by IRAS. On average in the atomic interstellar medium $\sim 15\%$ of the cosmic carbon is in small particles, PAH's or others, with less than a few hundred heavy atoms (Puget and Léger 1989). Based on this estimate, observed color variations imply that this fraction varies from place to place within molecular clouds from less than $\sim 5\%$ to more than half of the cosmic abundance.

It is not clear how one can explain such strong abundance variations. BFPH have proposed that they are related to the cycling of interstellar matter between the gas phase and grain surfaces. In their scenario small particles are a product of chemistry on grain surfaces. Regions of low $R(12,100)$ correspond to pieces of clouds where small particles are condensed onto grains, while high $R(12,100)$ are found where small particles condensed on grains and those formed out of photo-processed molecular ices are released to the gas phase through photo-desorption by UV photons (Draine and Salpeter 1979) or as the result of localized heating (Duley 1989). From the strength of the $3.4\mu\text{m}$ feature in the direction of the Galactic center Tielens and Allamandola (1987) estimate that 25 to 50% of the carbon along this line of sight is in organic mantles. The quantity of carbon observed to be in mantles is thus comparable to the amplitude of the cycling necessary to account for the color variations.

The existence of abundance variations on small scales imply that the evolution time-scale regarding the abundance of small particles must be comparable to the mixing time-scale of matter by turbulent motions within clouds. This correspondence is readily understandable in clouds where the density structure is controlled by transient compressions associated with turbulent motions. Recent observations at high angular resolution support such a picture for clouds with moderate gas column density ($A_v < \text{a few mag}$) (see Falgarone 1991 for a review). These observations have shown the existence, throughout clouds, of density peaks with $n_H \sim 5 \times 10^3 \text{ cm}^{-3}$, not massive enough to be bound by self-gravity. This density is also the one derived from molecular observations of moderate column density gas with no $12\mu\text{m}$ emission. For such a density, assuming a sticking probability of one, the condensation time scale of light molecules like H_2O is $3 \times 10^5 \text{ yr}$. For PAHs the condensation time scale depends on their relative velocity with respect to dust grains. Assuming a relative velocity of a few 10^3 cm s^{-1} (see Omont 1986) the time scale for condensation of PAHs is about an order of magnitude higher than that of small molecules. For a sticking probability of one, it is comparable to the mutual coagulation time scale among the smallest particles. The question which remains to be answered is to know whether the time spent by the gas in dense regions is long enough to permit significant condensation of gas species on grains. The answer may differ from cloud to cloud which would explain observed differences in colors between clouds.

If the IR color variations are related to the formation and destruction of mantles one expects that the abundance of small particles will depend on the frequency at which matter cycles between dense and diffuse regions compared with the time-

scales for condensation and detachment. In a cloud where matter cycles from diffuse to dense regions quickly relative to the detachment time-scale but slowly compared to the condensation time-scale large mantles will build up on grains and the abundance of small particles in the gas phase will drop. This would correspond to clouds of type (1) described in the morphology section. In the case where cycling time-scale is large compared to both condensation and detachment time-scales the abundance of small particles will be low in dense regions and normal or high in diffuse parts leading to the limb-brightening of colors observed in clouds of type (2). Finally a random distribution of colors as in clouds of type (3) should indicate that all time-scales are comparable. This interpretation of the data predicts that the color morphology of clouds is related to the internal velocity and density structure which may be tested by molecular line observations. Preliminary comparisons between IR and molecular observations do suggest such a relation (see Observational Properties). Other observations which would confirm the existence of abundance variations and test the connection between color variations and the cycling and processing of interstellar matter on grains have been suggested by BFPH. If these observations demonstrate this hypothesis it will imply that cycling of matter between gas phase and dust grains is more ubiquitous and rapid than previously thought.

Whichever it is, the physical process at the origin of the color variations needs to involve a large amount of material and to take effect on short time-scales to account for the observed properties. It is thus necessarily a key mechanism in the physical and chemical evolution of molecular clouds. IRAS images have revealed us a conspicuous sign of the evolution of interstellar matter in clouds which is very worth investigating further.

References

- Beichman, C., Wilson, R.W., Langer, W., and Goldsmith, P. 1988, *Ap. J.*, 332, L81.
- Bernard, J.P. 1990, Private Communication.
- Boulanger, F., Baud, B., and van Albada, G.D. 1985, *Astr. Ap.* 144, L9
- Boulanger, F., and Pérault, M., 1988, *Ap. J.* 330, 964.
- Boulanger, F., Falgarone, E., Helou, G., and Puget, J.L., 1989, in *Interstellar Dust Contributed Papers*, eds. A.G.G.M. Tielens and L. J. Allamandola, NASA CP-3036.
- Boulanger, F. 1989, *The Physics and Chemistry of Interstellar Molecular Clouds*, eds. G. Winnewisser and J. T. Armstrong, Springer Verlag, p. 30
- Boulanger, F., Falgarone, E., Puget, J.L., and Helou, G. 1990, *Ap. J.* 364, 136
- Chlewicki, G., and Laureijs, R.J., 1988, *Astr. Ap.* 207, L11.
- Désert, F.X., Boulanger, F., and Puget, J.L. 1990, *Astr. Ap.* 237, 215.
- de Vries, C.P., and Le Poole, R.S. 1985, *Astr. Ap.*, 145, L7.
- Draine, B.T., and Salpeter E.E. 1979, *Ap. J.* 231, 438.
- Draine, B.T., and Anderson, N. 1985, *Ap. J.*, 292, 494.
- Duley, W.W. 1989, *The Physics and Chemistry of Interstellar Molecular Clouds*, eds. G. Winnewisser and J.T. Armstrong, Springer Verlag, p. 353.
- Falgarone, E. 1991, *From Ground-based to Space-borne Submillimeter Astronomy*, eds. N. Longdon and B. Kaldeich, ESA Publ.
- Heiles, C., Reach, W.T., and Koo, B.C., 1988, *Ap. J.* 332, 313.
- Laureijs, R.J., Mattila, K., and Schnur, G. 1987, *Astr. Ap.* 184, 269.
- Laureijs, R.J., Chlewicki, G., Clark, F.O., 1988. *Astr. Ap.* 192, L13.
- Laureijs, R.J., Chlewicki, G., Clark, F.O., and Wesselius, P.R., 1989, *Astr. Ap.* 220, 226.
- Laureijs, R.J. 1989, Ph. D. University of Groningen.
- Laureijs, R.J., Clark, F.O., and Prusti, T. 1990, *Ap. J.* in press.
- Leene, A. 1985, *Astr. Ap.*, 154, 295.
- Omont, A. 1986, *Astr. Ap.*, 169, 159.
- Puget, J.L., Léger, A., and Boulanger, F. 1985, *Astr. Ap.*, 142, L19.
- Puget, J.L. 1989, *Interstellar Dust*, eds. L. J. Allamandola and A.G.G.M. Tielens, Kluwer, p. 119.
- Puget, J.L., and Léger, A., 1989, *Ann. Rev. Astr. Ap.*, 27, 161.
- Tielens, A.G.G.M., and Allamandola, L.J. 1987, *Interstellar Processes*, eds. D. Hollenbach and R. Thronson, Reidel, p. 397.
- Weiland, J.L., Blitz, L., Dwek, E., Hauser, M.G., Magnani, L., and Rickard, L.J. 1986, *Ap. J.*, 306, L101.